AFRL-RH-WP-TR-2009-0075

Height Reconstruction from Radar Shadow

Yunbao Huang
Xiaoping Qian
Illinois Institute of Technology
3300 South Federal Street
Chicago IL 60616-3793

Brian Tsou
Warfighter Interface Division
Supervisory Control Interfaces Branch

April 2009

Final Report for May 2007 to November 2008

Air Force Research Laboratory
711th Human Performance Wing
Human Effectiveness Directorate
Warfighter Interface Division
Supervisory Control Interfaces Branch
Wright-Patterson AFB OH 45433-7022

NOTICE AND SIGNATURE PAGE

Using Government drawings, specifications, or other data included in this document for any purpose other than Government procurement does not in any way obligate the U.S. Government. The fact that the Government formulated or supplied the drawings, specifications, or other data does not license the holder or any other person or corporation; or convey any rights or permission to manufacture, use, or sell any patented invention that may relate to them.

This report was cleared for public release by the 88th Air Base Wing Public Affairs Office and is available to the general public, including foreign nationals. Copies may be obtained from the Defense Technical Information Center (DTIC) (http://www.dtic.mil).

AFRL-RH-WP-TR-2009-0075 HAS BEEN REVIEWED AND IS APPROVED FOR PUBLICATION IN ACCORDANCE WITH ASSIGNED DISTRIBUTION STATEMENT.

//signed//
BRIAN H. TSOU
Work Unit Manager
Warfighter Interface Division

//signed//
DANIEL G. GODDARD
Chief, Warfighter Interface Division
Human Effectiveness Directorate
711th Human Performance Wing
Air Force Research Laboratory

This report is published in the interest of scientific and technical information exchange, and its publication does not constitute the Government's approval or disapproval of its ideas or findings.

REPORT DOCUMENTATION PAGE

Form Approved
OMB No. 0704-0188

1. REPORT DATE *(DD-MM-YYYY)*	2. REPORT TYPE	3. DATES COVERED *(From - To)*
23-04-2009	Final	05/14/07 – 11/28/08

4. TITLE AND SUBTITLE
Height Reconstruction from Radar Shadow

5a. CONTRACT NUMBER
F33615-01-D-3105

5b. GRANT NUMBER

5c. PROGRAM ELEMENT NUMBER
62202F

6. AUTHOR(S)

Yunbao Huang*
Xiaoping Qian*

Brian Tsou **

5d. PROJECT NUMBER
7184

5e. TASK NUMBER
09

5f. WORK UNIT NUMBER
71840911

7. PERFORMING ORGANIZATION NAME(S) AND ADDRESS(ES)

Illinois Institute of Technology*
3300 South Federal Street
Chicago IL 60616-3793

8. PERFORMING ORGANIZATION REPORT NUMBER

9. SPONSORING / MONITORING AGENCY NAME(S) AND ADDRESS(ES)
Air Force Materiel Command**
Air Force Research Laboratory
711th Human Performance Wing
Human Effectiveness Directorate
Warfighter Interface Division
Supervisory Control Interfaces Branch
Wright-Patterson AFB OH 45433-7022

10. SPONSOR/MONITOR'S ACRONYM(S)
711 HPW/RHCI

11. SPONSOR/MONITOR'S REPORT NUMBER(S)
AFRL-RH-WP-TR-2009-0075

12. DISTRIBUTION / AVAILABILITY STATEMENT
Approved for public release; distribution unlimited.

13. SUPPLEMENTARY NOTES

88 ABW/PA Cleared 06/22/2009; 88ABW-09-2766.

14. ABSTRACT

When using radar to transit a dark rugged area, the pilot needs to recognize dangerous obstacles ahead from radar images. Since the radar image is displayed as range versus azimuth, the obstacles cannot be easily seen, and the heights of obstacles are especially difficult to determine. It is important to detect potential obstacles such as tall buildings so that the aircraft can avoid collision. Therefore, we investigated height reconstruction methods (including multi-scale wavelet and histogram analysis) on the extracted radar shadows formed by obstacles. Preliminary results indicated that height construction was successful even with long thin shadows embedded in a noisy radar image.

15. SUBJECT TERMS
radar shadow, obstacle height

16. SECURITY CLASSIFICATION OF:			17. LIMITATION OF ABSTRACT	18. NUMBER OF PAGES	19a. NAME OF RESPONSIBLE PERSON
a. REPORT	b. ABSTRACT	c. THIS PAGE			Brian Tsou
U	U	U	SAR	16	19b. TELEPHONE NUMBER *(include area code)*

Standard Form 298 (Rev. 8-98)
Prescribed by ANSI Std. Z39.18

This page intentionally left blank.

TABLE OF CONTENTS

LIST OF FIGURES

THIS PAGE INTENTIONALLY LEFT BLANK

SUMMARY

When using radar to transit a dark rugged area, the pilot needs to recognize dangerous obstacles ahead from radar images. Since the radar image is displayed as range versus azimuth, the obstacles cannot be easily seen, and the heights of obstacles are especially difficult to determine. It is important to detect potential obstacles such as tall buildings so that the aircraft can avoid collision. Therefore, we investigated height reconstruction methods (including multi-scale wavelet and histogram analysis) on the extracted radar shadows formed by obstacles. Preliminary results indicated that height construction was successful even with long thin shadows embedded in a noisy radar image.

1.0 INTRODUCTION

When using radar to transit a dark rugged area, the pilot needs to recognize dangerous obstacles ahead from radar images [1, 2, 3, 4, 5]. Since the radar image is displayed as range versus azimuth, the obstacles cannot be easily seen, nor can their heights be easily determined. It is important to detect potential obstacles such as tall buildings so that the aircraft can avoid collision. For example, in the picture on the left of Figure 1, the pilot needs to fly over or around the towering smokestack in the foreground. Its corresponding radar image, on the right of Figure 1 – in B-scope, does not clearly show the smokestack or even approximate its height.

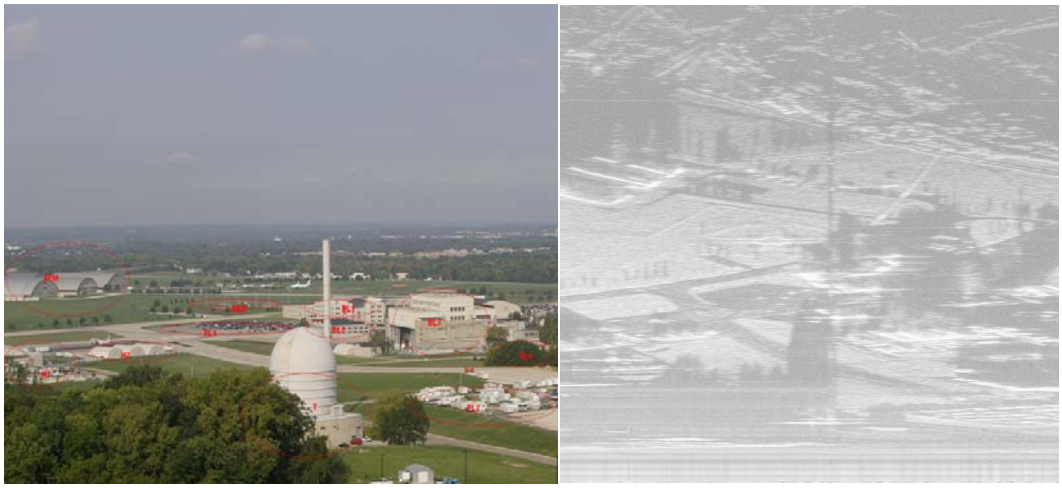

Figure 1: Left: Tall buildings, natural objects, and long-thin smokestack; Right: Radar image

The radar returns can be displayed as the range to targets on an oscilloscope – a display often referred to as the range scope or A-scope. In order to provide an improved spatial sense of the scene, a B-scope displays the range along the vertical axis and its corresponding radar azimuth (angle) on the horizontal axis in a 2-D display. It is a range vs. angle display of the scene. However, as the above example shows, it does not convey an object's height. An alternative − the C-scope −displays elevation (angle) information on the vertical axis. This angle vs. angle display presents a perspective view of the scene as in ordinary optical imagery, e.g., a human eye, camera, etc. Since all objects need to be perspectively projected in C-scope, the object height information need to be first determined from the radar returns. Tall objects can reflect the radiating energy back and cause a black shadow (receiving no illumination) behind its structure. The length of the shadow represents the object's height above the flat terrain. Such information has in the past been used to infer the object heights [6, 7, 8]. Thus, the overall objective of this project is to

1) Convert a B-scope image to a C-scope image so that human operators can easily understand the image content.

2) Extract the shadow formed by obstacles on a B-scope image.

3) Reconstruct the height from the recognized shadow onto the C-scope image [9, 10].

This project mainly focuses on the last two issues.

2.0 METHODS

As shown in Figure 2, using the ***input*** from a B-scope image, the following steps are performed:

1) **multi-scale and histogram analysis –**
   (a) de-noise the B-scope image,
   (b) recognize the weak shadow signal, *e.g.*, the smokestack attached to the tower in B-scope, along the azimuth direction, and
   (c) extract edges from the de-noised B-scope image.

2) **noise-based shadow extraction –** extract shadow intervals because there is no signal return except noise in the shadow area.

3) **height reconstruction from shadow –** extract height information based on geometric principles in shadow projection.

4) **height conversion from B-scope to C-scope –** convert and display the height in the C-scope.

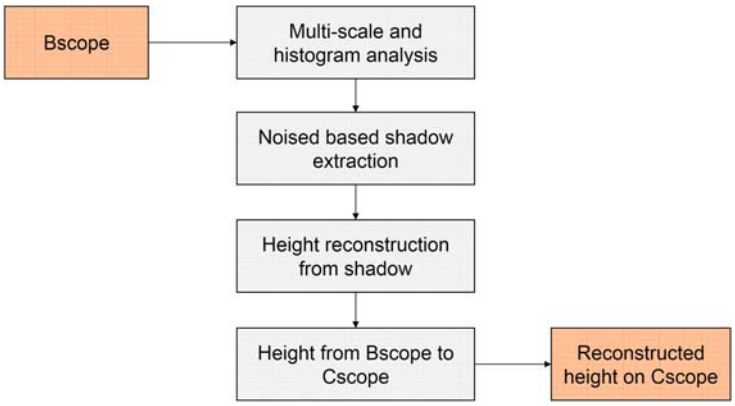

Figure 2: Flowchart of shadow extraction and height reconstruction

The ***output*** is the reconstructed height on the converted C-scope image. The detailed techniques are given in the following sections.

2.1 Multi-scale and Histogram Analysis

In Figure 3, the big building such as a tower has a clear and wide shadow, which can be easily recognized and extracted. However, it is not so easy to isolate the thin and noisy shadow of the smokestack, which is especially important for flight safety. We apply *multi-scale wavelet* and *histogram analysis* on the B-scope image to filter noise and isolate the weak signal, *i.e.*, the thin and noisy shadow.

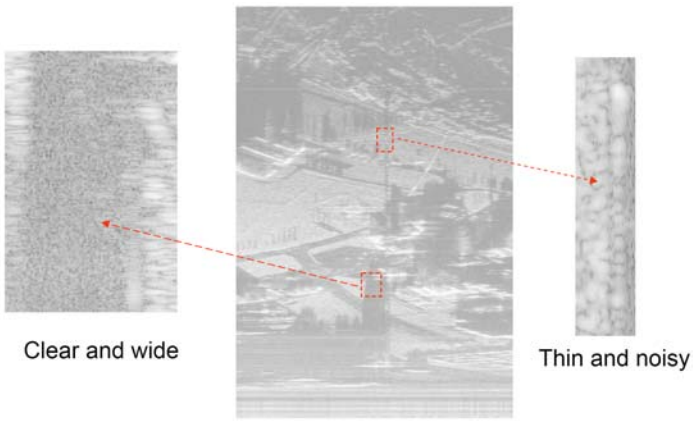

Figure 3: Different shadows on the *tower* B-scope image

Figure 4 gives the flowchart of such multi-scale and histogram analysis. For a given B-scope image, we first apply multi-scale analysis to filter the noisy image through a wavelet de-noise tool and obtain a de-noised B-scope image. With the de-noised image, we detect the edge features and histogram the edge features along the azimuth direction. As the result, we obtain an edge-information-based image, in which it is easy to detect the smokestack. The synthetic example below illustrates how this multi-scale wavelet and histogram analysis can achieve better results with a weak or noisy signal.

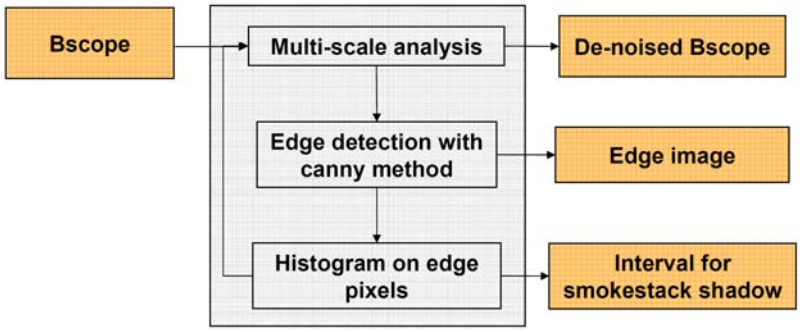

Figure 4: Flowchart of multi-scale and histogram analysis on a B-scope image

In

Figure 5, the shadow in the image can be easily detected via the edge histogram when the noise scale is lower than 0.5. Noisy image is first computed by subtracting the original B-scope from its de-noised image. The noise scale is the RMS value of the noisy image. However, when the noise scale equals 0.9, the shadow from the image could not be reliably extracted and the edges histogram analysis is not helpful. In such a case, we then conduct multi-scale wavelet analysis to extract the shadow information. The approach is demonstrated next.

Noise scale	Noisy image	Extracted edges	Histogram of edges
0	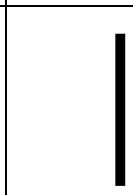	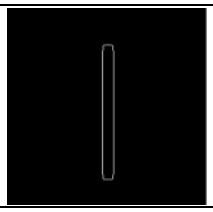	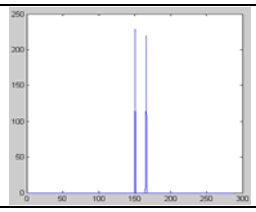
0.01	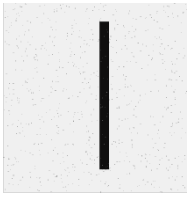	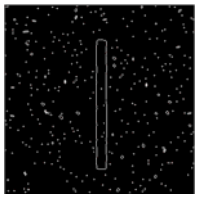	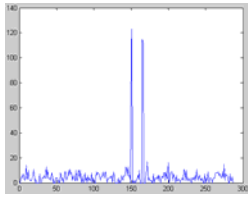
0.1	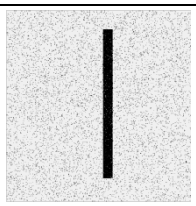		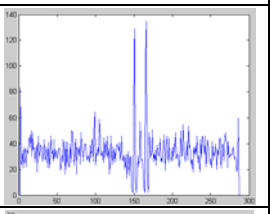
0.5	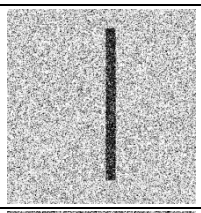	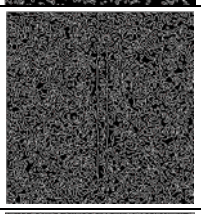	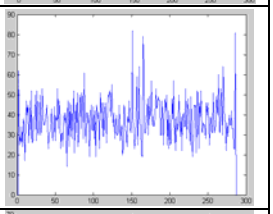
0.9	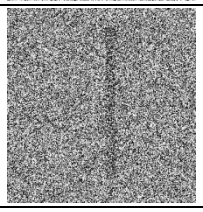	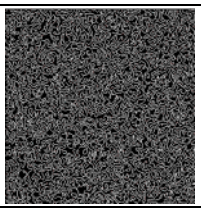	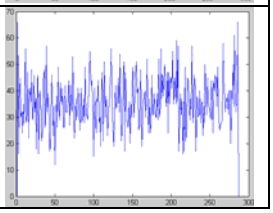

Figure 5: Signal recognition through edge histogram analysis

As can be seen in Figure 6, the shadow on the image can be detected from the edge histogram of the image after five levels of multi-scale wavelet analysis. Therefore, we demonstrated

1) multi-scale wavelet analysis can be used to remove the noise from the original noisy image and enhance the signal, and

2) multi-scale and edge histogram analysis can effectively detect the thin and long weak signal on a noisy image.

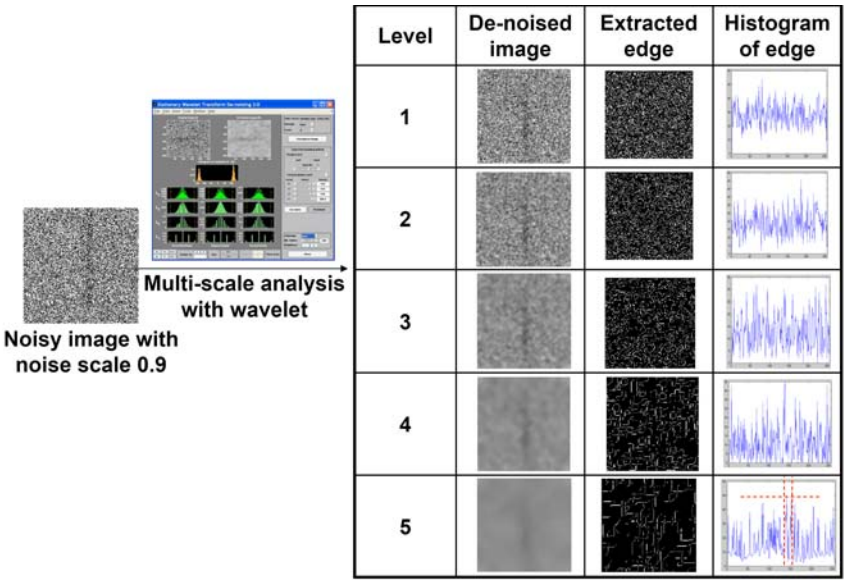

Figure 6: Multi-scale and histogram analysis on the image with noise scale 0.9

Therefore, we select the multi-scale wavelet and histogram analysis to extract the weak shadow signal in the B-scope image. The example below depicts the steps of the multi-scale wavelet and histogram analysis performed on our B-scope image.

In Figure 7, the large size B-scope image (600×16384) is decomposed into four smaller size B-scope images (600×4096), and multi-scale wavelet analysis (3 levels) is performed for each sub-image; these sub-images are then recombined. Finally, the edge information is extracted using the Canny edge detection tool. From the edge histogram, the weak signal of the long thin smokestack can now be easily recognized.

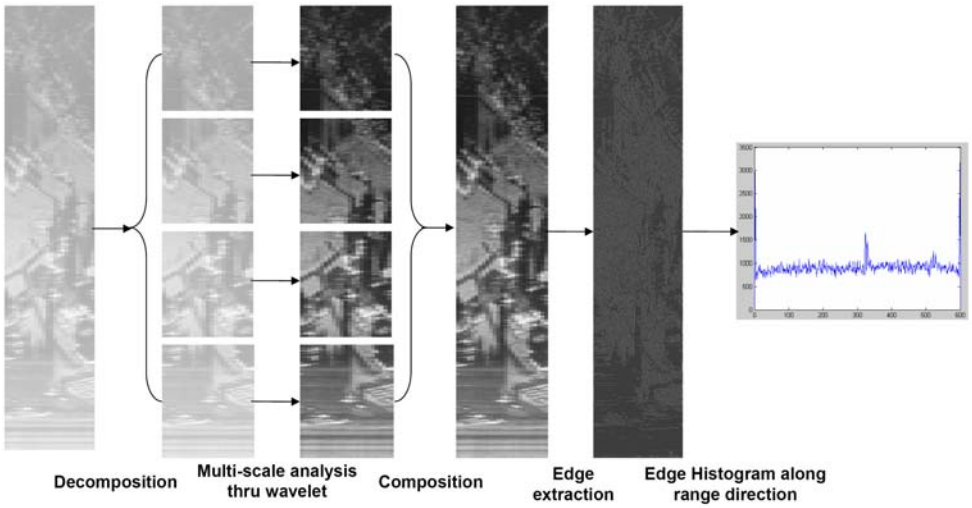

Figure 7: Multi-scale and histogram analysis on a B-scope image

2.2 Noise-based Shadow Extraction

Figure 8 describes the geometric projection principle of the overlay and shadow in a B-scope image, which also leads to three sharp changes of the image intensity: from background to overlay, from overlay to shadow, and from shadow to background. The sharp changes of intensity imply that there are edge features present, and the shadow intervals along the elevation direction are between those edge features. In addition, the shadow is the noisy interval that has no returned signal. Such characteristics form the *noise-based shadow extraction approach*. The following flowchart in the next figure shows the noise based shadow extraction approach.

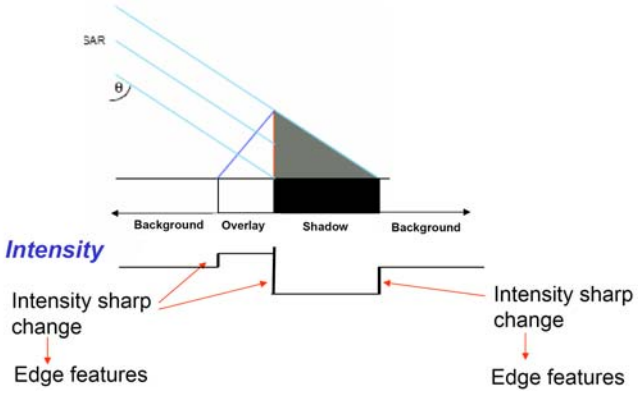

Figure 8: Edge features extraction from the intensity change on the B-scope

As shown in Figure 9, three steps are included to extract shadow intervals:

1) noise computation by subtracting the de-noised B-scope from the original B-scope image (Figure 10),

2) extract the possible shadow intervals between two edges on the edge image, and

3) validate the shadow interval with noise thresholds θ and θ'.

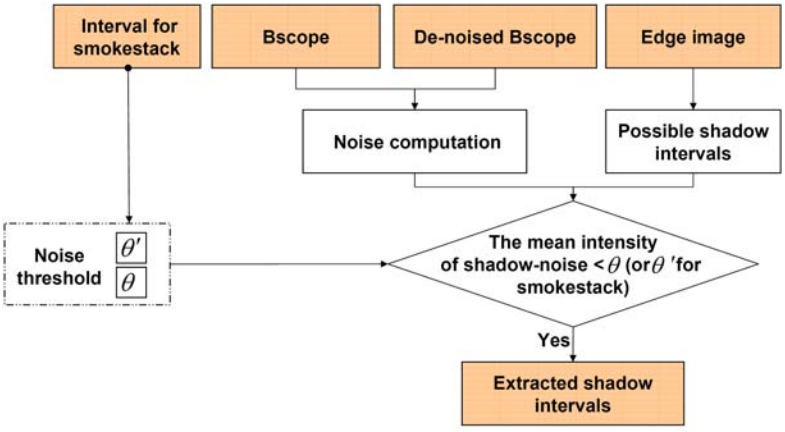

Figure 9: Flowchart of noise-based shadow extraction approach

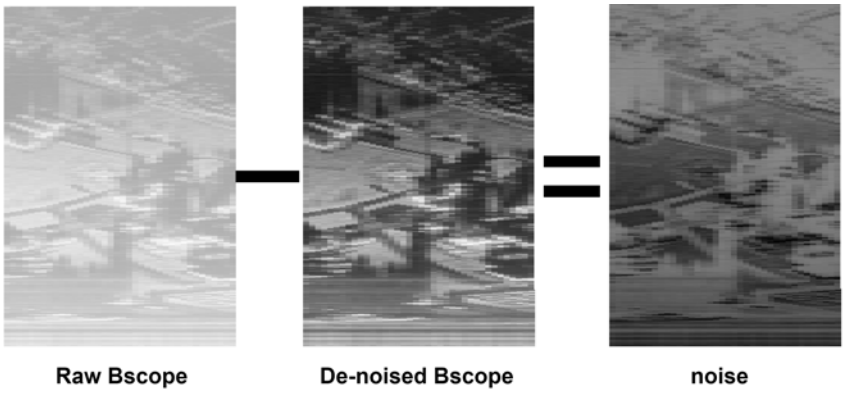

Figure 10: Noise computation by subtracting de-noised B-scope from raw B-scope

Based on the computed noise and possible shadow interval, we can extract the true shadow intervals with noise thresholds θ and θ'.

The noise thresholds θ and θ' can be selected in the following way:

1) compute the mean value of noise,

2) θ start from zero and increase until the reconstructed height looks more realistic,

3) θ' then starts from θ and increases until the reconstructed height of smokestack looks more realistic.

During the noise thresholds θ and θ' selection process, the height needs to be reconstructed, as detailed in the next section.

2.3 Height Reconstruction from Extracted Shadow

From the geometric relationship between the height H, slant length L, L_1, the *Altitude* between radar and ground, and angle φ in Figure 11, we have

$$\varphi = \arcsin\left(\frac{Altitude}{L}\right), \text{ and } H = (L - L_1)\sin(\varphi). \quad (1)$$

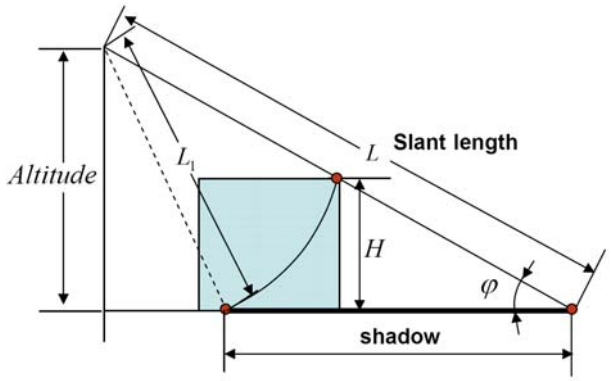

Figure 11: Geometric relationship between the height and shadow

Based on slant length, we use Eq. 1 to reconstruct height for each shadow interval.

2.4 Conversion from B-scope to C-scope

This section describes the procedure used to convert the height from the B-scope to the C-scope.

As shown in Figure 12a, there is a mapping interval in B-scope to C-scope conversion, *i.e.*, the intensity of one pixel in the C-scope is mapped to the mean value of a mapping interval on the B-scope. When the pixel marking the base of the obstacle is mapped to the correct pixel in the corresponding C-scope display, the height will be accurately reconstructed as shown in Figure 12b. However, if it is not correctly mapped as in Figure 12c, the obstacle height will not be accurately portrayed (the height should be H', not H). The following approach (shown in Figure 13) is therefore used to convert the height in the B-scope to C-scope.

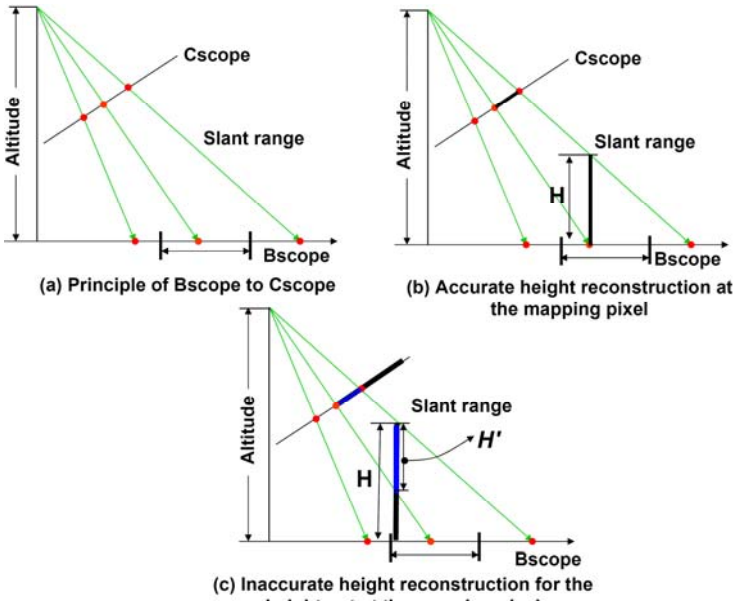

Figure 12 : Height conversion from B-scope to C-scope

As shown in Figure 13, H is the actual height of the building, H' is the height of the obstacle that should be mapped to the C-scope. In the triangle T shown in Figure 13, we have

$$\frac{L_1}{\sin(90^\circ - \varphi_1)} = \frac{H'}{\sin(\varphi_1 - \varphi)}. \tag{2}$$

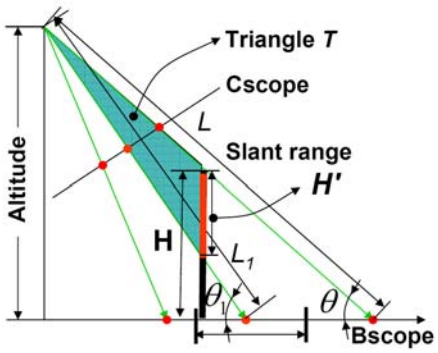

Figure 13: "Far height" reconstruction after the mapping interval expanding

Thus, from Eq. 2, the height H' can be calculated from

$$H' = \frac{L_1 \sin(\varphi_1 - \varphi)}{\cos(\varphi_1)}. \tag{3}$$

3.0 RESULTS AND DISCUSSION

Figure 14 shows the converted height as displayed in the C-scope (with noise thresholds $\theta' = 9.6 \times 10^6$ and $\theta = 2.8 \times 10^6$). Comparing to the visual scene in Figure 14a, it is clear that, while the B-scope (Figure 14b) display misrepresents the smokestack height and its location, the tall buildings, trees in the foreground, and the thin weakly imaged smokestack in the converted C-scope (Figure 14c) have all been successfully reconstructed.

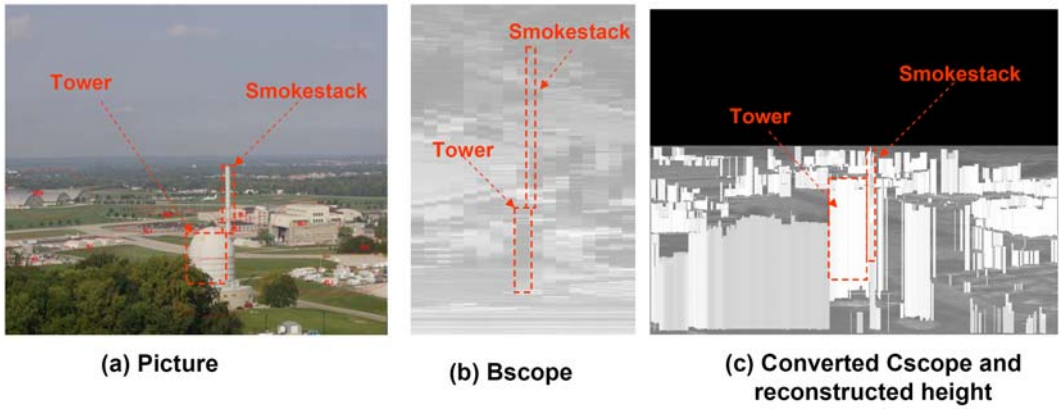

Figure 14: Reconstructed heights from extracted shadows

4.0 CONCLUSIONS

In this report, we documented the following analysis:

- Edge features can be used to extract possible shadow intervals, which are then used to reconstruct the height in C-scope.
- Multi-scale wavelet analysis can be used to (a) filter noise and (b) enhance the weak features (e.g., smoke stack detection) along the azimuth direction.
- Edge histograming can be applied to different scales of the image to extract the smoke stack.
- Noise is computed by subtracting B-scope from its de-noised image and this estimated noise is then employed to eliminate the non-shadow interval.
- Accurate height reconstruction can be performed during B-scope to C-scope conversion.

The combination of multi-scale wavelet and edge histogram analysis is successful in identifying the features even when they are long, thin and corrupted by noise.

5.0 REFERENCES

1. Pearson, R., Absi, A., Fetner, R., Tsou, B., and Anesgart, M. (2005) *Autonomous approach and landing capability (AALC) infrared (IR) comparison test* (AFRL-SN-WP-TR-2006-1009). Wright Patterson AFB, Ohio: Air Force Research Laboratory.
2. Pearson R. M., Absi, A. E. & Tsou, B. H. (2004) "Fused Millimeter Wave Radar/Infrared (MMWR/IR) Autonomous Landing System (ALS) demonstration," AFRL-SN-WP-TR-2004-1026, Wright-Patterson AFB, OH.
3. Sweet, B. T. and Tiana, C., "Image processing and fusion for landing guidance," Enhanced and Synthetic Vision, SPIE Vol. 2736, pp. 84 – 95, 1996.
4. Takacs, B., Sadovnik, L., Manasson ,V., Wade, M., Klein, L. A., Wong, D., Kiss, B., Benedek, B. and Szijarto, G., "Real-time Visualization Using a 2D/3D Imaging MMWave Radar," SPIE Electronic Imaging, Real-Time Imaging VIII (EI13), San Jose, CA, Jan 18 -22, 2004.
5. Wiseley, P. L., "The Application of Head Up Displays to Reduce Both Controlled Flight into Terrain and Approach and Landing Accidents Through Enhanced Situational Awareness," IEE, Savoy Place, London WC2R OBL, UK, 2002.
6. Eineder, M. and Suchandt, S., "Recovering Radar Shadow to Improve Interferometric Phase Unwrapping and DEM Reconstruction," IEEE Transactions on Geoscience and Remote Sensing, pp. 2959 - 2962, Vol. 41, No. 12, Dec 2003.
7. Tupin, F., "Extraction of 3D information using overlay detection on SAR images," 2nd GRSS/ISPRS Joint Workshop on "Data Fusion and Remote Sensing over Urban Areas", pp. 72 - 76.
8. Soergel, U., Thoennessen, U., and Stilla, U., "Utilization of LIDAR DEM for SAR Image Analysis in Dense Urban Areas," (Layover and Shadow)
9. Stilla, U., Sorgel, U., and Thonnessen, U., "Geometric constraints for building reconstruction from InSAR data of urban areas,"
10. Balz, T., and Haalz, N., "SAR-Based 3D-Reconstruction of Complex Urban Environments,"

6.0 GLOSSARY OF TERMINOLOGY

A-scope: radar display of the range to targets along a scale.

B-scope: a 2-D "top down" representation of space, with the vertical axis typically representing range and the horizontal axis azimuth (angle).

C-scope: a "bull’s eye" view of azimuth vs. elevation.